Stopping power for low-velocity heavy ions: (0–1.0)-MeV/nucleon Mg ions in 17 (Z = 22–79) elemental solids

K. Arstila, J. Keinonen, and P. Tikkanen
Accelerator Laboratory, University of Helsinki, Hämeentie 100, SF-00550 Helsinki, Finland
(Received 16 October 1989; revised manuscript received 4 December 1989)

The stopping power for ^{24,26}Mg ions in 17 (Z = 22–79) elemental solids has been studied in the energy region 0–1.0 MeV/nucleon by application of the Doppler-shift attenuation method. At velocities $2v_0 < v < 5v_0$ (v_0 the Bohr velocity), the scaling factors 1.10 (Ti), 0.90 (V), 0.93 (Fe), 0.97 (Co), 0.99 (Ni), 1.03 (Cu), 1.05 (Ge), 1.05 (Nb), 1.15 (Mo), 1.05 (Pd), 1.08 (Ag), 1.09 (Hf), 1.07 (Ta), 1.05 (W), 1.05 (Re), 1.05 (Pt), and 0.96 (Au) to the commonly used empirical electronic stopping power by Ziegler, Biersack, and Littmark were determined to an accuracy of ±5%. At velocities $v < 2v_0$, much higher electronic stopping power and different velocity dependence than predicted by the empirical model were obtained. The electronic stopping power was determined to an accuracy of ±5%. The reduction of the nuclear stopping power due to the polycrystalline structure of the slowing-down materials was taken into account in the deduction of the electronic stopping power.

I. INTRODUCTION

Experimental information on the electronic stopping power obtained in several measurements during recent years has been used by Ziegler *et al.*[1] to construct an empirical model on the basis of the Brandt-Kitagawa theory.[2] The experimental information was utilized to obtain the values of the model parameters. This empirical model is now commonly used in all cases where the electronic stopping power is needed to predict or interpret results of various measurements with heavy-ion beams.

For the parametrization of the electronic energy loss, the velocity dependence was treated differently in three velocity regions. In the velocity region $v < v_F$ (Fermi velocity $v_F \sim$ Bohr velocity $v_0 = c/137$ in the solids), the stopping power was assumed to be proportional to the velocity. In the velocity region $v > 3\ v_F$, the electronic energy loss was obtained by describing the ion as a Thomas-Fermi atom and using Bohr's stripping model to explain the energy loss by the equivalent experimental energy loss of protons. In the medium-velocity region $v_F < v < 3\ v_F$ where the Thomas-Fermi atom no longer represents the almost neutral heavy ion, the electronic stopping power and its velocity dependence were obtained by taking into account the charge-density distribution of electrons and the shielding of the nucleus. The velocity of crossover from low-velocity stopping to medium-velocity stopping was determined from the lower limits of validity of the empirical parameters describing the ionization level of ions in solids and of the Brandt-Kitagawa theory. The stopping power at the crossover velocity determined then the constant of proportionality at lower velocities.

Excluding our recent results,[3,4] there are to our knowledge no experimental data available in the literature that could be used to test the velocity dependence of the empirical electronic stopping power in the low-velocity region $v < 2v_0$. The obvious reasons are experimental difficulties and difficulties to take into account a realistic nuclear stopping power. Therefore, it is not known how well the electronic energy loss is reproduced by the model at low velocities. Without an experimental confirmation the validity of the empirical model is ambiguous, e.g., in applications in materials physics where the range and deposited energy distributions of MeV energy heavy ions are needed and in the Doppler shift attenuation (DSA) measurements in nuclear physics.[5–7]

The aim of this work was to test the empirical electronic stopping power at low velocities, $v < 2v_0$. The electronic stopping power has been studied in this work in the velocity region $v = 0–5v_0$ by measuring DSA data of ^{24,26}Mg ions in 17 (Z = 22–79) elemental solids and by comparing the experimental data with computer simulations. In the DSA measurements, the velocity of recoiling nuclei at the moment of the γ-ray emission depends on the stopping power of the slowing-down material. The line shape of a γ peak in the γ-ray spectrum shows the velocity distribution of the recoiling nuclei at the moment of the γ-ray emission. For a known lifetime the stopping power can be tested. The well-established mean lifetimes of the first excited states in ^{26}Mg ($\tau = 661 \pm 28$ fs, $E_x = 1809$ keV) and ^{24}Mg ($\tau = 1970 \pm 40$ fs, $E_x = 1369$ keV) are good standards for the study of the stopping power.[8,9] To our knowledge the DSA method is at the moment the only technique to experimentally test the electronic stopping power and its velocity dependence at very low velocities. In some previous works where this method has been used to study electronic stopping power at high velocities, $v > 2v_0$, the nuclear stopping power and the large-angle scattering have not been taken into account with an accuracy that would make the use of the data meaningful for an evaluation of the electronic stopping power at low velocities, $v < 2v_0$.[10,11] In this work, the reduction of the nuclear stopping due to the polycrystalline structure of the slowing-down materials was taken

into account on the basis of experimental data. The Monte Carlo calculations[7] removed the uncertainty due to Blaugrund's approximation[12] in the description of large-angle scattering.

II. EXPERIMENTAL PROCEDURE

The targets were prepared by implanting 3×10^{17} 40-keV $^{12}C^{+}$ ions/cm^2 into polycrystalline Ti, Co, Mo, Nb, Hf, Ta, and Re backings at the isotope separator of the laboratory. Also very low-density carbon targets on all the backings given in Table I were prepared.[6] The thicknesses of the mechanically polished backings used in both groups of targets were more than 0.5 mm.

In the DSA measurements, the recoiling magnesium ions and the excitation of the 1.81-MeV ^{26}Mg and 1.37-MeV ^{24}Mg levels were produced in the reactions $^{12}C(^{16}O,2p)^{26}Mg$ and $^{12}C(^{16}O,\alpha)^{24}Mg$. Beam energies of 24.0 and 27.0 MeV for ^{16}O were chosen to obtain the initial recoil velocities of $4.4v_0$ and $4.7v_0$, respectively, of the compound ^{28}Si nuclei. Due to the reaction kinematics the initial velocities of the recoiling ^{24,26}Mg ions had broadened distributions. The velocity distributions were determined experimentally by the use of the low-density carbon targets, Fig. 1. At the ^{16}O energies of 24.0 and 27.0 MeV the velocity regions were $3.9-4.9v_0$ and $4.1-5.3v_0$ for the recoiling ^{26}Mg ions and $2.5-6.3v_0$ and $2.7-6.7v_0$ for the recoiling ^{24}Mg ions, respectively. The slowing-down conditions are illustrated in Fig. 2 for ^{26}Mg ions in Ta. Due to the broad initial velocity distributions of Mg ions, this method could not be used in a detailed study of the velocity-dependent correction to the empirical stopping power. For that reason the thin low-density carbon targets, giving much higher γ-ray yields than the implanted targets, were used to find out the scaling factors to the empirical electronic stopping power at velocities below the initial velocity distributions and especially to study electronic stopping power at velocities $v<2v_0$. Figure 3 shows that at ion velocities below the initial ve-

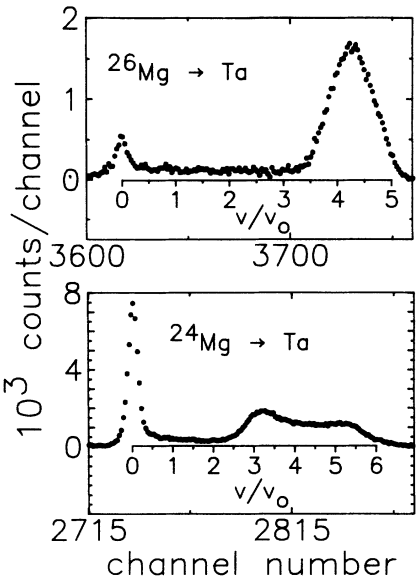

FIG. 1. Portions of γ-ray spectra recorded in the DSA measurements with thick low-density carbon target on the Ta backing. The broad parts of the line shapes at high recoil velocities illustrate the initial recoil velocities of ^{26}Mg (upper part) and ^{24}Mg ions (lower part) produced at $E(^{16}O)=24$ MeV.

TABLE I. Correction factors f_e to the empirical electronic stopping power[1] at ion velocities above the critical velocity v_c, and the proportionality constants k of the velocity proportional electronic stopping power at ion velocities below v_c for ^{24,26}Mg ions in different elemental solids.

Element	Z	v_c/v_0[a]	f_e[b]	k[c] (keV/nm)
Ti	22	1.7(0.73)	1.10	1.29
V	23	2.2(0.58)	0.90	1.59
Fe	26	2.8(0.78)	0.93	1.70
Co	27	2.4(0.72)	0.97	1.81
Ni	28	2.9(0.49)	0.99	1.72
Cu	29	2.7(0.68)	1.03	1.63
Ge	32	2.4(0.76)	1.05	1.20[d]
Nb	41	1.6(0.70)	1.05	1.64
Mo	42	1.6(0.39)	1.15	1.91
Pd	46	1.7(0.35)	1.05	1.82
Ag	47	2.0(0.39)	1.08	1.61
Hf	72	2.1(0.83)	1.09	1.39
Ta	73	1.8(0.61)	1.07	1.57
W	74	1.6(0.42)	1.05	1.78
Re	75	1.9(0.69)	1.05	1.92
Pt	78	2.2(0.42)	1.05	1.96
Au	79	2.4(0.30)	0.96	1.63

[a]The corresponding value according to the empirical model is given in parentheses.
[b]The absolute uncertainty of the factor is ±5%.
[c]The electronic stopping power is taken to be proportional to the ion velocity, i.e., $dE/dx=k(v/v_0)$, at velocities $v<v_c$. The uncertainty is ±5%.
[d]The electronic stopping power is taken to be $dE/dx=k(v/v_0)^{0.75}$, see the text.

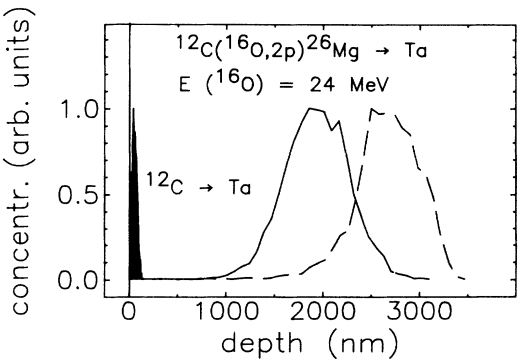

FIG. 2. Computer simulations of the range profile of 40-keV ^{12}C ions in Ta (dashed area), the depth distribution of recoiling ^{26}Mg ions at the moment of the γ-ray emission (solid line), and the range profile of ^{26}Mg ions (dashed line).

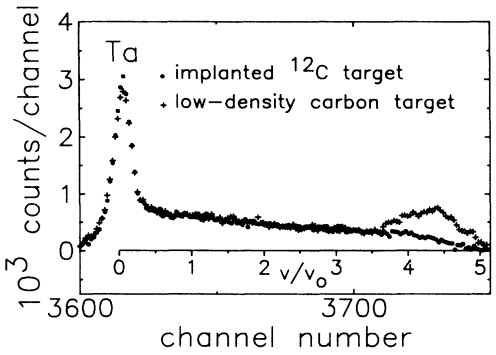

FIG. 3. Comparison of the 1.81-MeV γ-ray line shapes obtained with the thin low-density carbon and implanted ^{12}C target for ^{26}Mg ions slowing down in Ta, $E(^{16}\mathrm{O})=24$ MeV.

locity distribution, identical γ-ray line shapes are obtained with the implanted and thin low-density carbon targets.

The O^{5+} beams of 0.5–1.5 μA were supplied by the tandem accelerator EGP-10-II of the laboratory. The ion beam was focused to a 3×3 mm^2 spot on the target. A vacuum better than 1 μPa in the target chamber was used to prevent carbon buildup on the target surface during the measurements.

The γ-ray spectra were measured with both the implanted ^{12}C and the low-density carbon targets and stored in an 8K channel memory. The dispersions were 0.5–1.0 keV/channel. The γ rays were detected with a coaxially drifted PGT 120 cm^3 Ge(Li) detector (efficiency 21.8%). The energy resolution (FWHM) of the detection system was 2.2 keV at $E_\gamma=1.3$ MeV and 3.5 keV at $E_\gamma=2.6$ MeV. The stability of the spectrometer was checked with a ^{208}Tl γ-ray source and ^{40}K laboratory background. The detector was located at the angle of 0° to the beam direction and subtended a solid angle of 400 msr. At 0° the Doppler broadening of γ-ray peaks is most prominent and the effects due to the finite detector size are minimized. The count rate due to the low-energy γ rays and x rays was limited by the use of a 4-mm lead absorber between the target and the detector. The energy and efficiency calibration of the γ-ray detector was done with ^{56}Co and ^{152}Eu sources[13,14] placed in the target position.

III. LINE-SHAPE ANALYSIS

The Doppler-broadened γ-ray line shapes were first corrected for the background. This was done by subtracting a shaped background which had the form of a running integral matched to the mean background levels below and above the peak. The experimental line shape was then corrected for the change of the detector efficiency in the energy region of the peak. An example of the experimental γ-ray lineshapes corrected for these effects is given in Fig. 4.

For the tests of the semiempirical stopping power values,[1] the Doppler-broadened γ-ray line shapes corresponding to the velocity spectrum of the recoiling ^{24,26}Mg ions at the moment of the γ-ray emission were produced by computer simulations.[5,15] The line shapes of the 1.81-MeV ^{26}Mg and 1.37-MeV ^{24}Mg γ-ray peaks depend mainly on the stopping powers of the slowing down materials and the lifetimes[8,9] of the 1.81-MeV ($\tau=661\pm28$ fs) ^{26}Mg and 1.37-MeV ($\tau=1970\pm40$ fs) ^{24}Mg levels. The measured line shapes were also affected by other effects which were taken into account in the simulations and are discussed in the following.

The stopping power of the slowing-down materials for the recoiling ^{24,26}Mg ions was described by the following equation:

$$\left[\frac{dE}{dx}\right]_{\mathrm{corr}}=f_n\left[\frac{dE}{dx}\right]_n+f_e\left[\frac{dE}{dx}\right]_e. \tag{1}$$

The uncorrected nuclear stopping power $(dE/dx)_n$ was derived by calculating the scattering angles of the recoiling ions directly from the classical scattering integral.[16] the interatomic interaction was derived from the Thomas-Fermi potential.[7,17] The correction factor f_n accounts for the stopping power reduction due to the microchanneling of the recoiling atoms in the polycrystalline backing material. This approach is based on the fact that in simulations of γ-ray line shapes[18] no significant differences have been obtained either using the polycrystalline structure and the interatomic potential[17] or the experimentally determined correction factors of the nuclear stopping power.[7] The value $f_n=0.75\pm0.15$ adopted in all the cases studied in this work, was based on direct measurements and systematic studies on the correction factor at low ($v<v_0$) velocities done in our laboratory.[7,19–28] The given error limits cover the scatter and uncertainties of different values. The uncertainty in the deduced electronic stopping power values due to the uncertainty of f_n will be discussed in the following.

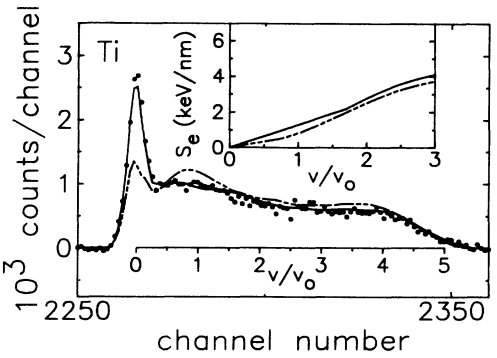

FIG. 4. Portion of a γ-ray spectrum illustrating the measured 1.81-MeV ^{26}Mg γ-ray peak for the Ti backing at $E(^{16}\mathrm{O})=27$ MeV. The target was the implanted ^{12}C target. The solid line shows the line shape obtained in the computer simulation with the corrected electronic stopping power. The dashed line illustrates the line shape for the empirical electronic stopping power. The corrected electronic stopping power S_e (solid line) and the empirical stopping power (dashed line) are illustrated at low velocities in the inset.

The uncorrected electronic stopping power $(dE/dx)_e$ was first calculated in the framework of the empirical model.[1] At velocities higher than about $3v_0$, the scaling factor f_e was used to reproduce the experimental line shapes. At lower velocities the values obtained for the scaling factor were not adequate for the description of the measured line shapes. In order to reproduce the line shapes at these velocities, the electronic stopping power was assumed to be proportional to the ion velocity in a larger velocity region than predicted by the empirical model. The deduction of the stopping power is described in Sec. IV.

Small corrections for the delayed feedings from upper states[9] to the 1.81-MeV ^{26}Mg and 1.37-MeV ^{24}Mg states were taken into account in the simulations. In the Monte Carlo simulations a realistic correction could be done. A simulated line shape was obtained as the sum of the shapes corresponding to the direct prompt and delayed populations of the state. The sum was weighted by the experimentally determined fractions of the populations. The line shape of the 1.81-MeV γ-ray peak was corrected for the (5±2)% and (10±3)% delayed feedings (relative to the intensity of the 1.81 MeV γ-ray peak) from the 4.32 MeV (τ=377±26 fs, Refs. 8 and 9) and 2.94-MeV (τ=134±25 fs, Refs. 8 and 9) states, respectively. The line shape of the 1.37-MeV γ-ray peak was corrected for the (10±3)%, (5±2)%, and (30±6)% feedings (relative to the intensity of the 1.37-MeV γ-ray peak) from the 7.62-MeV (1190±200 fs, Ref. 5), 5.24-MeV (95±5 fs, Ref. 5), and 4.12-MeV (33.1±2.6 fs, Ref. 5) states, respectively. The error limits of the intensities cover the differences obtained at $E(^{16}O)=24$ and 27 MeV.

The effect of the finite size of the γ-ray detector and the measured dependence of the detector efficiency on the angle between the γ-ray emission and the symmetry axis of the detector were taken into account in the simulations. The effect of the angular distribution of the γ rays could be accounted for by modifying the detector efficiency properly. The Doppler shift of an emitted γ ray was calculated up to the second order in the velocity of the recoiling ions.

The simulated γ-ray line shapes were convoluted with the experimental line shape, measured with a standard radioactive source, to account for the finite-energy resolution of the detector. The intensity of the simulated peak was required to be equal to the intensity of the experimental peak in the final χ^2 fit of the line shapes.

IV. RESULTS

The simulated γ-ray line shapes are illustrated in Figs. 4 and 5 for the empirical electronic stopping power[1] and the stopping power deduced in this work.

At velocities $v > 2v_0$, all the measured γ-ray line shapes were reproduced by scaling the empirical electron stopping power with the factors f_e given in Table I. Naturally that part of the γ-ray line shape that corresponded to the initial velocity distribution of the recoiling Mg ions was neglected in the fitting of the simulated line shapes with those obtained with the low-density carbon targets. The uncertainty ±5% of the correction factors arises

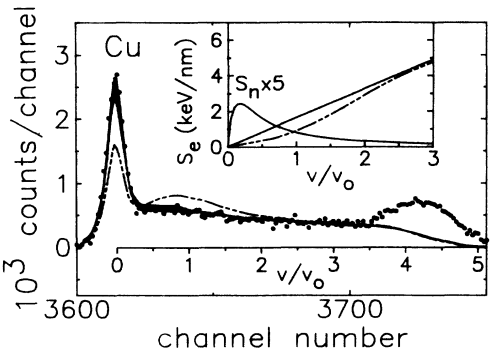

FIG. 5. As for Fig. 4, but for the Cu backing, low-density carbon target, $E(^{16}O)=24$ MeV, and to illustrate the effect of the nuclear stopping power on the line shape. The thick part of the solid line illustrates the difference between the line shapes obtained with the correction factors $f_n=0.5$ (the lower boundary at the stop peak and the upper boundary elsewhere) and 1.0 (the upper boundary at the stop peak and the lower boundary elsewhere). In the inset, the nuclear stopping power S_n corresponding to the scaling factor $f_n=0.75$ is also shown.

from the uncertainties of the mean lifetimes of the 1.81-MeV ^{26}Mg and 1.37-MeV ^{24}Mg states, the uncertainties due to the corrections of the simulated line shapes already described, and the statistical uncertainties. The uncertainty of the nuclear stopping power correction has a negligible effect on the uncertainty of f_e, see Sec. V.

The disagreement between the simulated and experimental line shapes observed for all the slowing-down materials at velocities $v < 2v_0$, indicated that the electronic energy loss is much higher and its velocity dependence different than predicted by the empirical model.[1] In order to reproduce the experimental γ-ray line shapes, the stopping power was assumed to be proportional to the ion velocity up to higher velocities than used in the empirical model. The highest velocity for the linear velocity dependence was called the critical velocity v_c. The values of v_c were found in the fitting of the experimental and simulated line shapes. The stopping power at v_c calculated from the corrected empirical stopping power, determined the constant of proportionality. The values of the proportionality constant k and the critical velocity v_c/v_0 are given in Table I. The deduced electronic stopping powers are illustrated for Ti and Cu in the insets of Figs. 4 and 5. The uncertainty ±5% of the deduced stopping power values arises from the same uncertainties as that of f_e. The uncertainty due to the nuclear stopping power will be discussed in Sec. V.

For the semiconductor band-gap target Ge the velocity dependence was taken to be $(v/v_0)^{0.75}$ according to Ref. 1. In connection and in test simulations of other line shapes with velocity dependences differing from the linear one, it was found that the deduced stopping powers are proportional to $(v/v_0)^{0.75}$ for Ge and to the ion velocity for the other solids within the uncertainty of the values obtained for k, i.e.,

$$(dE/dx)=k(v/v_0)^{0.75\pm0.07} \quad (2)$$

TABLE II. Results for the electronic stopping power (in MeV/mg cm^{-2}) for ^{24,26}Mg ions in 17 elemental solids. The absolute uncertainty is ±5%. Corrections for the nuclear stopping power have been applied.

v/v_0	Ti	V	Fe	Co	Ni	Cu	Ge	Nb	Mo	Pd	Ag	Hf	Ta	W	Re	Pt	Au
0.2	0.57	0.52	0.43	0.41	0.39	0.37	0.67	0.38	0.37	0.30	0.31	0.21	0.19	0.18	0.19	0.18	0.17
0.4	1.15	1.04	0.87	0.81	0.77	0.73	1.13	0.77	0.75	0.61	0.61	0.42	0.38	0.37	0.37	0.36	0.34
0.6	1.72	1.56	1.30	1.22	1.16	1.10	1.53	1.15	1.12	0.91	0.92	0.63	0.57	0.55	0.56	0.55	0.51
0.8	2.29	2.09	1.73	1.63	1.55	1.46	1.90	1.53	1.50	1.21	1.23	0.84	0.76	0.73	0.75	0.73	0.68
1.0	2.87	2.61	2.16	2.03	1.93	1.83	2.24	1.91	1.87	1.52	1.53	1.05	0.95	0.91	0.94	0.91	0.84
1.2	3.44	3.13	2.60	2.44	2.32	2.19	2.57	2.30	2.25	1.82	1.84	1.25	1.13	1.10	1.12	1.09	1.01
1.4	4.01	3.65	3.03	2.85	2.71	2.56	2.89	2.68	2.62	2.12	2.15	1.46	1.32	1.28	1.31	1.28	1.18
1.6	4.59	4.17	3.46	3.25	3.09	2.92	3.19	3.06	2.99	2.43	2.45	1.67	1.51	1.46	1.50	1.46	1.35
1.8	5.30	4.69	3.89	3.66	3.48	3.29	3.49	3.61	3.57	2.77	2.76	1.88	1.70	1.72	1.69	1.64	1.52
2.0	6.15	5.21	4.33	4.07	3.87	3.65	3.77	4.15	4.11	3.16	3.08	2.09	2.00	1.98	1.91	1.82	1.69
2.2	6.93	5.75	4.76	4.47	4.25	4.02	4.05	4.64	4.60	3.54	3.52	2.34	2.28	2.22	2.17	2.00	1.86
2.4	7.63	6.42	5.19	4.87	4.64	4.39	4.33	5.09	5.04	3.92	3.95	2.60	2.54	2.46	2.41	2.26	2.03
2.6	8.22	7.00	5.62	5.32	5.02	4.75	4.72	5.48	5.42	4.27	4.35	2.82	2.77	2.68	2.64	2.49	2.27
2.8	8.72	7.48	6.07	5.71	5.41	5.13	5.07	5.84	5.76	4.60	4.72	3.02	2.97	2.89	2.85	2.69	2.49
3.0	9.13	7.86	6.40	6.05	5.80	5.49	5.38	6.15	6.06	4.90	5.05	3.19	3.16	3.08	3.05	2.87	2.69
3.2	9.46	8.14	6.69	6.35	6.14	5.81	5.66	6.42	6.32	5.17	5.33	3.35	3.33	3.26	3.24	3.03	2.88
3.4	9.73	8.34	6.94	6.62	6.46	6.10	5.91	6.65	6.54	5.41	5.58	3.49	3.49	3.42	3.42	3.17	3.04
3.6	9.94	8.48	7.15	6.84	6.74	6.37	6.14	6.85	6.74	5.63	5.78	3.63	3.64	3.56	3.58	3.29	3.18
3.8	10.24	8.68	7.42	7.12	7.09	6.69	6.41	7.11	7.00	5.90	6.04	3.79	3.82	3.74	3.78	3.46	3.35
4.0	10.53	8.85	7.69	7.40	7.42	7.01	6.70	7.37	7.24	6.15	6.27	3.97	4.01	3.91	3.97	3.61	3.51
4.2	10.78	8.98	7.92	7.64	7.71	7.30	6.95	7.58	7.45	6.37	6.46	4.14	4.18	4.06	4.15	3.76	3.64
4.4	10.98	9.06	8.12	7.84	7.97	7.55	7.18	7.77	7.63	6.56	6.62	4.29	4.34	4.19	4.31	3.89	3.76
4.6	11.15	9.12	8.28	8.01	8.18	7.78	7.38	7.92	7.78	6.72	6.75	4.43	4.48	4.30	4.45	4.01	3.86
4.8	11.28	9.16	8.41	8.15	8.37	7.97	7.56	8.04	7.90	6.86	6.86	4.55	4.61	4.40	4.57	4.12	3.95
5.0	11.38	9.17	8.52	8.26	8.52	8.14	7.72	8.14	7.99	6.97	6.95	4.66	4.72	4.48	4.68	4.22	4.02

for Ge and

$$(dE/dx)=k(v/v_0)^{1.00\pm0.07} \quad (3)$$

for all the other solids studied in this work.

The deduced electronic stopping powers are summarized in Table II. The values were obtained by using the correction factors f_e and proportionality constants k given in Table I.

V. DISCUSSION

The results in Table I indicate that at velocities $v > v_c$ the empirical model predicts the electronic stopping in the elemental solids studied to within $\pm 10\%$, excluding Mo whose stopping power is 15% higher than predicted. At lower velocities, very strong deviations of the electronic stopping power from the predictions of the empirical model were obtained. Computer simulations of γ-ray line shapes for the f_n values of 0.5 and 1.0 indicated that at the velocities $v > v_0$ the uncertainty of the nuclear stopping power has a very small effect on the deduced electronic stopping power values, see Fig. 5. It is worth noting that due to the large-angle scattering of the recoiling Mg ions, the effect of the nuclear stopping power on the DSA line shape is considerably bigger than its portion in the total stopping power, inset of Fig. 5. At velocities much below v_0, the uncertainty of f_n could affect the velocity dependence of the electronic stopping power more than already assumed. However, up to now there is no evidence in the literature[1] that the assumption of the linear dependence is incorrect at very low velocities, i.e., $v < v_0/Z_1^{2/3}$ (Ref. 29) and the velocities given in Table I according to Ref. 1.

In our recent studies,[3,4] the empirical model[1] was found to describe the electronic stopping powers of Ta for $0-5.8v_0$ ^{23}Na, ^{24}Mg, ^{27}Al, ^{29}Si, ^{31}P, ^{34}S, ^{35}Cl, and ^{38}Ar ions within an uncertainty of $\pm 7\%$. Evidence on the velocity-dependent correction of the empirical electronic stopping was found in the cases of ^{23}Na and ^{24}Mg. Due to the very broad initial velocity distribution of recoiling ^{24}Mg ions the 1.37-MeV γ-ray line shape produced in the same nuclear reaction as in this work, was not sensitive enough for the deduction of a velocity dependent correction, see Fig. 1. In this work the 1.37-MeV ^{24}Mg γ-ray line shape was used only to control the correction factors obtained with the 1.81-MeV ^{26}Mg γ-ray line shape, corresponding to an almost optimal lifetime value for the studies of the electronic stopping power over a wide velocity region.

VI. SUMMARY

The empirical electronic stopping power[1] has been tested to an accuracy of $\pm 5\%$ for $0-5v_0$ Mg ions in 17 ($Z=22-79$) elemental solids by application of the DSA method in conjunction of well-established nuclear lifetimes and nuclear stopping powers. The results show that at ion velocities $v > v_c$ the electronic stopping power is reproduced by the empirical model within an uncertainty of $\pm 10\%$, excluding the 15% deviation for Mo. At velocities below the critical velocity v_c the empirical model was found to strongly underestimate the stopping power. The critical velocity used as a fitted upper limit to the linear velocity dependence, was observed to be 2–8 times higher than the velocity limit used in the empirical model for the linear velocity dependence of the stopping power. This resulted in a different velocity dependence of the electronic stopping power than predicted by the empirical model. No evidence for a deviation from the linear velocity dependence was found at ion velocities $v < v_c$, excluding the semiconductor material Ge for which the proportionality of $(v/v_0)^{0.75}$ was used in agreement with the empirical model.

ACKNOWLEDGMENTS

This work was supported by the Academy of Finland.

[1] J. F. Ziegler, J. P. Biersack, and U. Littmark, *The Stopping Powers and Ranges of Ions in Matter* (Pergamon, New York, 1985), Vol. 1.

[2] W. Brandt and M. Kitagawa, Phys. Rev. B **25**, 5631 (1982).

[3] J. Keinonen, A. Kuronen, M. Hautala, V. Karttunen, R. Lappalainen, and M. Uhrmacher, Phys. Lett. A **123**, 307 (1987).

[4] P. Tikkanen, Nucl. Instrum. Methods Phys. Res. B **36**, 103 (1989).

[5] J. Keinonen, P. Tikkanen, A. Kuronen, Á. Z. Kiss, E. Somorjai, and B. H. Wildenthal, Nucl. Phys. **A493**, 124 (1989).

[6] P. Tikkanen, J. Keinonen, V. Karttunen, and A. Kuronen, Nucl. Phys. **A456**, 337 (1986).

[7] J. Keinonen, in *Capture Gamma-Ray Spectroscopy and Related Topics (Knoxville, 1984)*, Proceedings of the Fifth International Symposium on Capture Gamma-Ray Spectroscopy and Related Topics, AIP Conf. Proc. No. 125, edited by S. Raman (AIP, New York, 1985), pp. 557–569.

[8] B. H. Wildenthal and J. Keinonen (unpublished).

[9] P. M. Endt and C. van der Leun, Nucl. Phys. **A310**, 1 (1978).

[10] J. S. Forster, T. K. Alexander, G. C. Ball, W. G. Davies, I. V. Mitchell, and K. B. Winterbon, Nucl. Phys. **A313**, 397 (1979).

[11] D. E. C. Scherpenzeel, G. A. P. Engelbertink, H. J. M. Aarts, C. J. Van der Poel, and H. F. R. Arciszewski, Nucl. Phys. **A349**, 513 (1980).

[12] A. E. Blaugrund, Nucl. Phys. **88**, 501 (1966).

[13] M. Hautala, A. Anttila, and J. Keinonen, Nucl. Instrum. Methods **150**, 599 (1978).

[14] *Table of isotopes*, 7th ed., edited by C. M. Lederer and V. S. Shirley (Wiley, New York, 1978).

[15] P. Tikkanen, Ph.D. thesis, University of Helsinki, 1989 (unpublished).

[16] H. Goldstein, *Classical Mechanics* (Addison-Wesley, Reading, MA, 1980), p. 74.

[17] M. Bister, M. Hautala, and M. Jäntti, Radiat. Eff. **42**, 210 (1979).

[18] M. Hautala, Phys. Rev. B **30**, 5010 (1984).

[19]J. Keinonen, A. Luukkainen, A. Anttila, and M. Erola, Nucl. Instrum. Methods **216**, 249 (1983).
[20]A. Luukkainen, J. Keinonen, and M. Erola, Phys. Rev. B **32**, 4814 (1985).
[21]A. Anttila, M. Bister, A. Luukkainen, Á. Z. Kiss, and E. Somorjai, Nucl. Phys. **A385**, 194 (1982).
[22]J. Keinonen, A. Luukkainen, and M. Bister, Nucl. Phys. **A412**, 101 (1984).
[23]M. Bister, A. Anttila, and J. Keinonen, Phys. Rev. C **16**, 1303 (1977).
[24]A. Anttila, S. Brandenburg, J. Keinonen, and M. Bister, Nucl. Phys. **A334**, 205 (1980).
[25]M. Bister, A. Anttila, and J. Keinonen, Phys. Lett. **53A**, 471 (1975).
[26]M. Luomajärvi, J. Keinonen, M. Bister, and A. Anttila, Phys. Rev. B **18**, 4657 (1978).
[27]J. Keinonen, M. Hautala, M. Luomajärvi, A. Anttila, and M. Bister, Radiat. Eff. **39**, 189 (1978).
[28]R. Lappalainen, Phys. Rev. B **34**, 3076 (1986).
[29]E. Fermi and E. Teller, Phys. Rev. **72**, 399 (1947).